ELSEVIER

Materials Science and Engineering A 375–377 (2004) 625–629

MATERIALS SCIENCE & ENGINEERING A

www.elsevier.com/locate/msea

Oxygen effects on glass formation of plasma arc sprayed $Cu_{47}Ti_{33}Zr_{11}Ni_8Si_1$ surface coatings

D.J. Sordelet [b,*], M.F. Besser [a]

[a] *Metals and Ceramics Sciences Program, Ames Laboratory, Ames, IA 50011, USA*

[b] *Metals and Ceramics Sciences Program, Ames Laboratory (USDOE), Department of Materials Science and Engineering, Iowa State University, 125 Spedding Hall, Ames, IA 50011-3020, USA*

Abstract

A series of thermal spray experiments were performed to produce $Cu_{47}Ti_{33}Zr_{11}Ni_8Si_1$ coatings from gas atomized powders synthesized with oxygen contents ranging from 0.125 to 0.79 wt.%. The amount of oxygen increased with decreasing particle size, which suggests the oxide is present as a surface film. Surface coatings were deposited using plasma arc spraying (PAS) in air and in an argon environment within an environmental chamber. The amount of amorphous phase was estimated for the gas atomized powders and plasma arc sprayed coatings. Despite the rapid solidification occurring during these two processing methods, substantial devitrification occurs in the high oxygen content powders and their associated coatings. Coatings deposited in air exhibit significantly more devitrification than their counterparts produced in the controlled environment chamber.

JCNS: M190-metallic glasses; A210-amorphous solids; D200-differential thermal analysis

Keywords: Metallic glass; Plasma arc spray; Devitrification

1. Introduction

The ability of a metallic glass-forming system to solidify from the molten state while avoiding significant nucleation or growth of crystalline phases is generally considered a function of cooling rate. Plasma arc spraying (PAS) can be used to deposit coatings of marginal metallic glass-forming alloys that retain some amorphous structure [1]. In addition to cooling rate sensitivity, previous work shows that the presence of oxygen in many amorphous alloys leads to heterogeneous nucleation of crystalline phases [2]. Even with oxygen contamination, it is possible to form an amorphous structure by either superheating the material to dissolve the oxide nucleation sites or by increasing the cooling rate such that crystallization is avoided.

The extremely high cooling rates associated with PAS are well suited for glass formation [3]. Coating material (usually powder) is fed to a spray gun where it is heated to the molten state and accelerated toward a substrate where the molten droplets hit, spread and solidify, forming a splat [4]. Each droplet solidifies in an independent event which allows very rapid cooling rates ($\sim 10^6\,K\,s^{-1}$). Repeated passes of the spray gun can build up coatings with thick cross-sections (>1 mm) of interlocking splats without significantly affecting the substrate or the previously deposited layers. The PAS techniques used in this study are especially useful because they operate using inert gas and can be used inside an environmental chamber to exclude oxygen and other contaminants from the process. Previous research has shown that an alloy of $Cu_{47}Ti_{33}Zr_{11}Ni_8Si_1$ can form a glass with a relatively high crystallization temperature (T_x) [1]. The addition of Si in this composition serves to reduce the sensitivity of the alloy's glass-forming ability (GFA) to the presence of contaminants such as O and C [2]. Because of its strong glass forming ability, this alloy was selected for the PAS experiments to emphasize the effects of O on glass formation rather than cooling rate.

2. Experimental method

A 40 kg master ingot was prepared and crushed in smaller pieces for five different gas atomization runs, which were

* Corresponding author. Tel.: +1-515-294-4713; fax: +1-515-294-8727.
E-mail address: sordelet@ameslab.gov (D.J. Sordelet).

0921-5093/$ – see front matter © 2003 Elsevier B.V. All rights reserved.
doi:10.1016/j.msea.2003.10.185

Table 1
Chemical analysis of gas atomized powders and PAS coatings

Sample label	Starting descriptor	Spray environment	Spray distance (cm)	Metallic composition (at.%)					Oxygen content (wt.%)	Amorphous fraction (%)
				Cu	Ti	Zr	Ni	Si		
Nominal composition				47	33	11	8	1		
Powder samples										
a				46.9	33.40	10.49	8.19	0.97	0.1292	99
b				46.6	32.77	11.00	8.94	0.63	0.2510	73
c				46.8	33.48	10.43	8.17	1.04	0.3298	71
d				46.9	32.47	10.84	9.23	0.57	0.3791	67
e				47.8	33.78	10.93	6.81	0.59	0.7130	52
Coating samples										
aA13	a	APS	13	45.4	34.6	10.9	8.2	1.0	3.448	49
aA23	a	APS	23	45.2	34.8	10.7	8.4	1.0	3.497	31
aA28	a	APS	28	44.2	35.4	10.9	8.5	1.0	4.904	31
aV13	a	VPS	13	47.0	33.4	10.5	8.1	1.0	0.3641	75
aV23	a	VPS	23	46.7	33.6	10.6	8.1	1.0	0.2827	78
aV28	a	VPS	28	47.4	33.1	10.4	8.0	1.0	0.2959	78
eA13	e	APS	13	44.7	36.1	11.8	6.9	0.6	4.439	22
eA23	e	APS	23	44.7	36.1	11.7	7.0	0.6	5.291	22
eA28	e	APS	28	44.1	36.4	11.8	7.1	0.7	6.166	20
eV13	e	VPS	13	47.9	33.9	10.9	6.8	0.6	0.841	36
eV23	e	VPS	23	47.9	33.9	10.9	6.8	0.6	0.8391	27
eV28	e	VPS	28	47.9	33.9	10.9	6.8	0.6	0.8133	34

conducted using previously developed parameters [5]. The atmosphere in each atomization run was controlled to vary the oxygen level of the $Cu_{47}Ti_{33}Zr_{11}Ni_8Si_1$ powders. The starting powders are labeled a, b, c, d and e in order of increasing O content, as defined in Table 1. All starting powders were sieved to a +45,−75 μm size fraction for characterization and PAS.

Coatings for this study were deposited with a Praxair SG-100 plasma arc spray gun (Praxair, Inc. Concord, NH) using operating parameters described in Ref. [3]. These parameters were chosen to increase particle velocity while limiting the heating of the feed material. Conditions such as these are typical for PAS of oxidation or vaporization sensitive materials. In order to examine the increase in the O level during the PAS process and its effect on the resulting coating structure, samples were sprayed using both air plasma spray (APS) (i.e., deposition in air) and vacuum plasma spray (VPS) (i.e., deposition at 40 kPa Ar in a chamber). Coatings formed by APS and VPS were deposited by rastering the plasma gun over a series of cleaned and grit-blasted 2 mm thick low carbon steel substrates at spray distances of 13, 23 and 28 cm away from the gun face. The thickness of the coatings was approximately 0.3 mm. Throughout this paper coatings are labeled with their starting powder (a–e), spraying environment (A for APS or V for VPS), and spray distance in cm (13–28). For example, a coating sprayed with powder a in air at a spray distance of 13 cm is labeled: aA13. A complete listing is given in Table 1.

The O content of all starting powders and coatings was measured by inert-gas fusion and is given in wt.% in Table 1 along with chemical analysis for all starting powders and selected coatings. Chemical analysis was done by inductively coupled plasma-atomic emission spectroscopy; metals-basis chemistry is reported in at.%. Thermal analysis was performed using differential scanning calorimetry (DSC) at $40\,K\,s^{-1}$ in flowing Ar. Using Perkin-Elmer Pyris software, the glass transition temperature (T_g), primary crystallization temperature (T_x) and the primary crystallization enthalpy (ΔH_{x1}) were estimated where applicable. The amount of crystalline phases present was estimated by the ratio of ΔH_{x1} for a sample to that of a specimen of the same composition, which was assumed to be fully amorphous as determined in a previous work [5]. X-ray diffraction (XRD) was performed on all coatings and starting powders using Cu Kα radiation. The polished cross-sections of coatings were examined using scanning electron microscopy (SEM) and energy dispersive spectroscopy (EDS). Additionally, a sample of coating eA13 was fractured in situ in a scanning auger microscope (SAM) to look for chemical segregation and O enrichment, particularly at splat (i.e., particle) boundaries.

3. Results and discussion

The starting compositions of all powders are close to that of the nominal composition of $Cu_{47}Ti_{33}Zr_{11}Ni_8Si_1$, Table 1. As reported earlier [5], the O content of $Cu_{47}Ti_{33}Zr_{11}Ni_8Si_1$ gas atomized powders increases with decreasing particle size, which suggests that O exists as a surface layer. A portion of the DSC results from the starting powders and applicable coatings are also presented in Fig. 1. As the O level increases in the starting powders, the onset of T_{x1} slightly

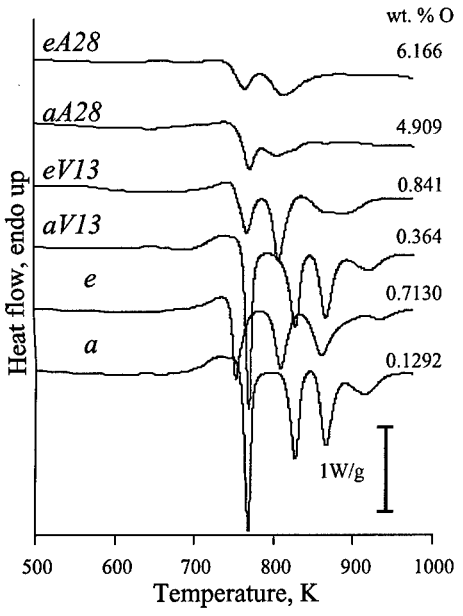

Fig. 1. DSC thermograms from starting powders a and e and PAS coatings formed with these powders using APS (aA28 and eA28) at 28 cm and VPS (aV13 and eV13) at 13 cm spraying distances, respectively.

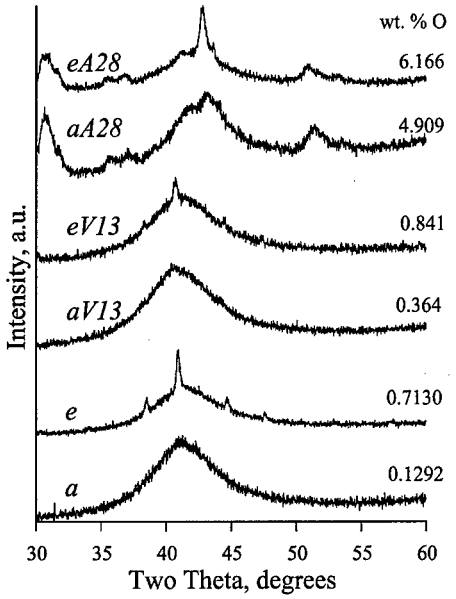

Fig. 2. X-ray diffraction patterns from starting powders a and e and PAS coatings formed with these powders using APS (aA28 and eA28) at 28 cm and VPS (aV13 and eV13) at 13 cm spraying distances, respectively.

decreases. For example powders a and e show onset temperatures for T_{x1} of 758 and 744 K, respectively. Presumably this reflects the increasing ease of crystallization in the presence of higher fractions of a crystalline phase within the as-atomized powders. Table 1 displays the dramatic reduction in the amorphous phase content with increasing oxygen. Note, the devitrification pathway of the $Cu_{47}Ti_{33}Zr_{11}Ni_8Si_1$ powders, Fig. 1, does not change from what has been reported [6] as the O level increases, but only shows a decrease in the total crystallization enthalpy.

XRD results indicate obvious peaks of crystalline diffraction for both powders and coatings that are higher in oxygen, while in the lower O samples there is no clear evidence of crystalline structure. Fig. 2 shows XRD patterns from the lowest and highest O contents for the powders and coatings. Powder *e* exhibits the initial devitrification phase that has been observed during continuous heating of this metallic glass [6]. The VPS coating formed with powder e also shows the emergence of the same crystalline phase within the remaining amorphous matrix. In contrast to the crystalline phases that nucleate and grow from the amorphous phase, additional crystalline phases are observed in coatings deposited in air. Coatings aA28 and eA28, which were formed at a very long spraying distance, 28 cm, contain oxides that yield the Bragg peaks seen at lower 2θ values in Fig. 2. This correlates with the higher O contents of these coatings, Table 1. The observed increase in crystalline phase contents of coatings with a higher O content, and more dramatically those sprayed in air are supported by the DSC results shown in Fig. 1. Powder a and coating aV13 show a clear T_g and a large ΔH_{x1}, whereas powders and coatings having higher O contents show no discernable T_g and smaller primary crystallization enthalpies. As observed with the starting powders, all coatings show a decrease in the amorphous content with increasing O.

Along with a decrease in amorphous content, coatings with higher O exhibit chemistry changes as a loss of Cu and Ni and a relative enrichment in Ti, Table 1. These chemical changes are seen only in the APS coatings, which were the highest in O. Backscattered electron images of the coatings show darkened regions in the APS coating that are not seen in the VPS sample, Fig. 3. Elemental mapping by EDS indicates these darker areas are Cu deficient. No correlation between O and these dark areas was seen using EDS. The higher vapor pressure of Cu [7] relative to the other elements in this alloy supports the idea of selective vaporization during plasma spraying. Since the vaporization is not seen in VPS, where the lower pressure should facilitate Cu loss, it is likely that the change is an O-assisted vaporization of a volatile Cu-oxide, which would only occur in air. Additionally, a SAM image of a fracture surface from coating eA13 shows a splat boundary that exhibits a shell, Fig. 4. This shell shows a smooth fracture surface commonly seen in crystalline materials while the interior of the particle shows the vein-like fracture surface associated with stress-induced fracture of amorphous materials [8]. A higher level of oxygen was seen by Auger spectroscopy at the shell compared to the areas showing the amorphous fracture pattern. This provides an indication that the gas atomized powders oxidize in flight, forming an oxide skin as seen in Fig. 4. These surface oxides may promote crystallization upon cooling, and more so during subsequent heating in the DSC experiments by a heterogeneous nucleation route. Moreover, the compositional changes that must occur in the material adja-

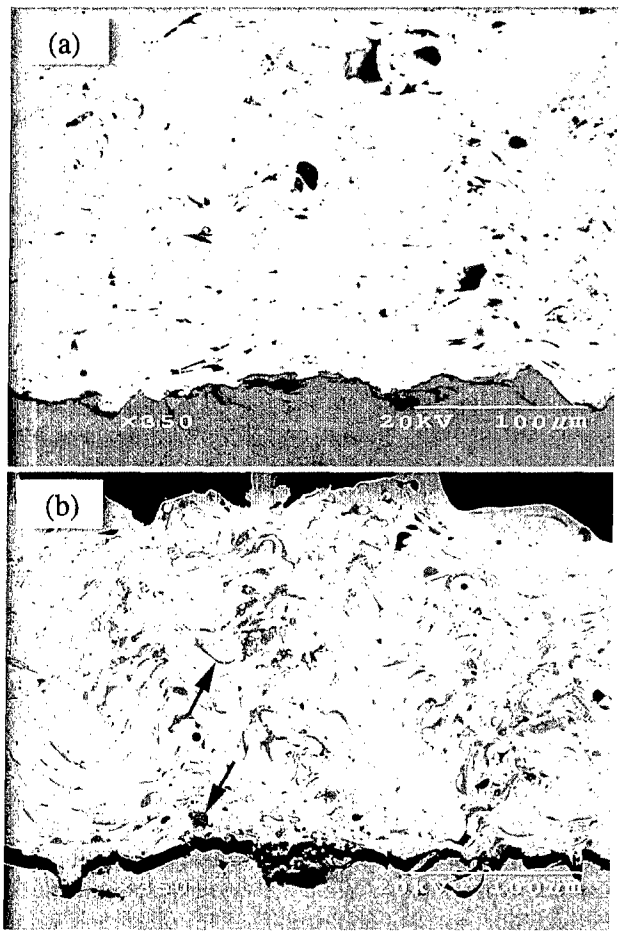

Fig. 3. BSE micrographs of PAS coatings (a) aV13 and (b) aA13 (see Table 1 for coating label descriptions). The arrows show the darkened Ti- and Zr-rich areas.

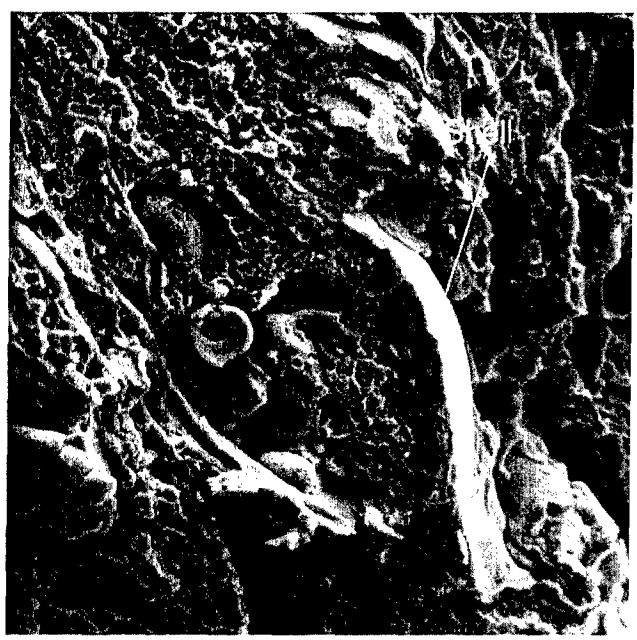

Fig. 4. SAM micrograph from and PAS coating eA13 revealing an O-rich shell around an amorphous-appearing splat along a fracture surface.

cent to the oxide skin (e.g., depletion of Ti or Zr) may also lead to a chemistry that has a lower glass forming ability or a higher tendency to crystallize upon heating. The DSC data represent a bulk measurement, but as indicated by the SAM results, oxidation and associated increased devitrification tendencies may be occurring much more locally in the PAS coatings, as compared to materials where oxygen is distributed much more homogeneously. This may partially explain why some samples in this study still have a measurable amorphous content compared to samples of the same alloy prepared by conventional casting techniques, which fail to form a glass with lower O contamination levels [9]. It is likely that the high cooling rates during PAS also extend the latitude for glass formation in the presence of higher O levels.

4. Conclusion

This study has shown that it is possible to deposit coatings of gas atomized $Cu_{47}Ti_{33}Zr_{11}Ni_8Si_1$ powders containing various levels of oxygen contamination using plasma arc spray methods. The structure of the coating was found to depend primarily on the spray environment, with an argon atmosphere producing the higher amorphous content in coating samples for a given starting powder. The oxygen content of the coatings reflected the relative levels of the oxygen contamination in the starting powders.

The analysis of the starting powders displayed oxygen contents ranging from 0.125 to 0.79 wt.%. It was shown that higher oxygen levels lead to more crystalline structure in the starting powders as determined by XRD and DSC. This trend was found to be true for both the starting powders and for the plasma sprayed coatings. Chemical composition for all starting powders was very close to the nominal alloy composition. Chemical changes in the coatings involved the loss of Cu in coatings where high levels of oxidation were found.

Acknowledgements

This was supported by the United States Department of Energy (USDOE),Office of Science (OS), Office of Basic Energy Sciences (BES), through Iowa State University under Contract W-7405-ENG-82.

References

[1] K. Kishitake, H. Era, F. Otsubo, J. Therm. Spray Technol. 3 (1996) 283.
[2] H. Choi-Yim, R. Busch, W.L. Johnson, J. Appl. Phys. 83 (1998) 7993.
[3] D.J. Sordelet, P. Huang, M.F. Besser, E. Lepecheva, ASM Int. Thermal Spray Surface Engineering via Applied Research, 2000, p. 851.
[4] H. Herman, Sci. Am. 256 (9) (1988) 112.

[5] D.J. Sordelet, E. Rozhkova, P. Huang, P.B. Wheelock, M.F. Besser, M.J. Kramer, M. Calvo-Dahlborg, U. Dahlborg, J. Mater. Res. 17 (2002) 186.
[6] D.J. Sordelet, M.J. Kramer, M.F. Besser, E. Rozhkova, J. Non-Cryst. Solids 290 (2001) 163.
[7] R.E. Honig, D.A. Kramer, Vapor Pressure Curves of the Elements, RCA Laboratories, Princeton, NJ.
[8] C.J. Gilbert, V. Schroeder, R.O. Ritchie, Metall. Mater. Trans. A 30A (1999) 1739.
[9] W.L. Johnson, MRS Bull. 24 (1999) 42.